Journal of Molecular Structure 1283 (2023) 135262

Contents lists available at ScienceDirect

Journal of Molecular Structure

journal homepage: www.elsevier.com/locate/molstr

Shock wave recovery experiments on poly-crystalline tri-glycine sulfate – X-ray and Raman analyses

A. Sivakumar[a], A. Saranraj[b], S. Sahaya Jude Dhas[c], T. Vasanthi[d], V.N. Vijayakumar[d], P. Sivaprakash[e], V. Pushpanathan[f], S. Arumugam[e], Lidong Dai[a,*], S.A. Martin Britto Dhas[g,*]

[a] Key Laboratory of High-temperature and High-pressure Study of the Earth's Interior, Institute of Geochemistry, Chinese Academy of Sciences, Guiyang, Guizhou, China 550081
[b] Department of Physics, Government Arts and Science College for Women, Barugur, Krishnagiri, Tamilnadu, India - 635 104
[c] Department of Physics, Kings Engineering College, Sriperumbudur, Chennai, Tamilnadu, India 602 117
[d] Department of Physics, Condensed Matter Research Laboratory, Bannari Amman Institute of Technology, Sathyamangalam, Tamil Nadu, India 638 401
[e] Centre for High Pressure Research, School of Physics, Bharathidasan University, Tiruchirapalli, Tamilnadu, India 620 024
[f] Department of Chemistry, Dr. M.G.R. Government Arts and Science College for Women, Villupuram, Tamil Nadu, India 605 602
[g] Shock Wave Research Laboratory, Department of Physics, Abdul Kalam Research Center, Sacred Heart College, Tirupattur, Vellore, Tamil Nadu, India 635 601

ARTICLE INFO

Article history:
Received 15 December 2022
Revised 14 February 2023
Accepted 28 February 2023
Available online 1 March 2023

Keywords:
Shock waves
Tri-glycine sulfate
Phase transition
NLO crystals

ABSTRACT

Recent reports of shock wave experiments on non-linear optical (NLO) crystals have demonstrated outstanding results. Suitable candidates are currently being studied for industrial applications. For the present experiment, we have chosen tri-glycine sulfate (TGS) for the investigation of the structural properties after shock wave loaded conditions by employing X-ray diffraction and Raman spectroscopic measurements. The observed diffraction and spectroscopic patterns of the test polycrystalline sample reveal that the test sample does not undergo any crystallographic phase transition. But, there are several additional shoulder peaks observed and Raman measurements show that a few Raman bands appear while some disappear by the impact of shock waves due to the re-orientational effect of glycine molecules. The observed interesting results are discussed.

1. Introduction

Shock-wave-induced investigation on properties of materials has emerged to be one of the prominent and promising scientific approaches that can enable an understanding of the stabilities of materials under the action of high-pressure and high-temperature environments. Since shock-wave impacts can simultaneously provide multiple effects such as high tension, high stress, high temperature and high-velocity impact, research on shock waves in materials science has gained significant momentum thereby attracting researchers cutting across various fields in recent years [1–5]. On the one hand, shock-wave-induced investigations, which have been carried out so as to unearth the properties of materials that are either crystalline or non-crystalline, have provided an alternative way to understand the predictable and unpredictable behavior of materials so that it could be possible to bring about new structural models of materials. On the other hand, shock-wave-assisted investigations on properties of materials are capable of authenticating the pathway to find high shock-resistant materials for technologically important applications such as radiation monitoring, earth exploration, aerospace, nuclear power plant and thermal protecting systems [6,7]. At the time of shock-wave propagation into the specimen, lots of changes in physical and chemical properties can occur that have been very well documented in recent years' reports [8–10]. Moreover, some of the materials have experienced the phenomenal behavior of phase transformation due to the impact of shock waves that have been already witnessed [11,12] and a few materials have exhibited structural stable properties against the shock wave impacts [13,14]. As it is known from the literature on interactions with shock waves, functional material properties such as electrical, optical, magnetic and thermal properties can be changed with respect to the crystallographic phase and degree of crystalline nature of the material. If the changes are induced in the crystallographic structures and degree of crystallinity by the effect of dynamic shock waves, the efficiency of devices would be at crossroads. The device engineers have put high demand on the researchers' work with the requirements such that the device materials should have high structural stability, high efficiency and a long lifetime against the harsh environments. Hence, the researchers working on shock waves continue to expend a tremen-

* Corresponding authors.
E-mail addresses: dailidong@vip.gyig.ac.cn (L. Dai), martinbritto@shctpt.edu (S.A.M.B. Dhas).

https://doi.org/10.1016/j.molstruc.2023.135262
0022-2860/

dous amount of effort to find high shock-wave-resistant materials and understand the role of shock waves in materials science.

The shock tube is recognized as one of the simplest tools that are being used to select the right candidate for the above-mentioned applications. Using a shock tube, we can generate high-pressure (up to several MPa) environments in laboratories [15]. For this study, special attention has been applied to investigate the effect of shock waves on optically transparent NLO materials since they are highly used in the applications of high power laser, micro-electronic devices, frequency converters, infrared (IR) detectors etc. [16]. In our earlier publications, we have investigated the crystalline stability of a few NLO crystals such as ammonium dihydrogen phosphate (ADP) [17] and potassium dihydrogen phosphate (KDP) [18]. Though these two crystals possess polymorphic nature with respect to temperature and pressure, the applied shock waves do not lead to any phase transitions. However, we have observed some interesting behaviors at shocked conditions within the same crystallographic crystal system. Fascinatingly, in the case of ADP poly-crystalline samples, its pyramidal face has experienced high degree of crystalline perfection while shock waves are loaded because of the occurrence of dynamic recrystallization and the observed results are shown by powder X-ray diffraction analysis [17]. On the other hand, in the case of KDP poly-crystalline samples, they exhibit a few additional crystalline peaks such as (204), (324) which appear and disappear according to the rate of exposed shock pulses [18]. Moreover, Zhukova et al., 2009 have examined the structural properties of super-conducting material of poly-crystalline MgB_2 at 65 GPa pressure and found the occurrence of micro-distortions [19]. For the present research article, another interesting ferroelectric NLO material namely triglycine sulfate (TGS), has been selected in polycrystalline form in order to perform the shock-wave-impact study since it has a wide array of literature over the past 70 years. TGS is being used for technological applications such as sensors, energy harvesters, micro-electronic devices, infrared detectors, non-volatile ferroelectric random-access memory, astronomical telescopes, radiation monitoring and earth exploration. Moreover, it possesses interesting structural properties with respect to pressure and temperature. TGS crystal has two crystallographic phases, monoclinic ($P2_1$) and monoclinic ($P2_1/m$). Interestingly, these two phases are non-centro symmetric and centro-symmetric, respectively and are ferroelectric and para-electric in nature, respectively [20–24]. Compared to the existing contributions on crystal growth of TGS and their characterizations, the behavior of TGS at high pressure is not completely understood. Looking into the few available literature reports of the high pressure materials science and crystallography of TGS crystal, the present investigation could add more scientific content for the significance of TGS. On the one hand, Andriyevsky et al., (2007) have performed first-principles calculations (DFT- CASTEP codes) and observed loss of ferroelectric behavior at 7.7 GPa pressure because of the space group changing from $P2_1$ to $P2_1/m$ [25]. On the other hand, Stankowsk et al., (2009) have demonstrated the phase change of ferroelectric to paraelectric at 2.4 GPa owing to the reduction of the concentration of ferroelectric domains [26]. Kobayashi et al., (2002) have found that a new high-pressure phase of TGS exists at 2.5 GPa and the respective tentative P-T phase diagram has been also proposed [27]. Eisuke et al., (2003) have also found similar results (high-pressure phase of TGS) at 2.5 GPa [28]. Enhancement of spontaneous polarization has been found at 76 k bar, 165k bar, and 218 k bar by Stankowski et al. [29]. From the literature survey of the static high-pressure-related research articles, the behavior of the title sample is quite known so that it has to be well understood. Hence, the title crystal is a worthy candidate to be investigated at dynamic shock wave impact conditions. In an earlier publication, we have investigated the influence of exposed shock waves on the optical properties of TGS crystal ($P2_1$ phase) and found that there is a reduction of the optical transmittance with respect to the number of shock pulses [30]. In the present experiment, we have investigated the crystallographic phase stability of $P2_1$ - TGS poly-crystalline samples with the shock wave of Mach number 2.2 by X-ray diffraction and Raman spectroscopic techniques (Mach number is the ratio of the velocity of generated waves to the velocity of the local acoustical waves).

1.1. Crystal growth

The test crystal was grown by the vacuum-assisted Sankaranarayanan–Ramasamy (VASR) method such that the crystallographic and analytical studies have been already reported by our research group [30,31]. A good quality seed crystal was mounted properly at the bottom of an ampoule so that the preferred plane (001) could grow facing the top of the ampoule. In order to prepare the growth solution, the test crystal of good quality obtained from the slow evaporation method was made into fine powder form using a mortar and pestle. Then, the powder was stirred thoroughly with distilled water to obtain the saturated solution which was filtered and transferred into the ampoule to the full capacity without disturbing the position of the seed crystal. Due to the concentration gradient, the test crystal was started growing along the (001) plane. After a month, the test crystal of unidirectional nature was harvested and it was powdered using a mortar such that the obtained powder was used for the shock wave recovery experiment. In total, four samples of equal measure have been prepared for the present experiment such that, out of the four, one has been kept as the control and the other three samples for the shock-wave-treatment.

1.2. Shock wave loading methodology

Shock waves were generated by a tabletop Reddy tube which was in-house designed and upgraded in our laboratory. The principle, working methodology and shock-wave-loading technique have been discussed in the previous articles [32,33]. Briefly, a gradual increase of air pressure in the driver section is maintained by an air compressor such that the diaphragm in the shock tube ruptures thereby it leads to the generation of a shock wave which is enabled traveling along the axis of the driven section from where it is directed towards the sample holder. The required samples to be tested are to be placed one by one sequentially in the sample holder which is in general kept 1cm away from the open end of the driven section. Consequently, the required different numbers of shock pulses are loaded on each of the test samples with a time interval of 5 s between every shock exposure. 100 number of shock pulse represents that a particular sample is loaded with 100 times by the shock pulse of a specific Mach number. Soon after the shock wave loading experiment is completed, the control and shock wave loaded samples are sent for the required analytical studies. For the present experiment, 50,100 and 150 shocks have been applied to the three chosen samples, respectively. The applied single pulse shock wave has a transient pressure of 2.0 MPa. After the shock-wave-loading process, the test samples have been sent for the required characterizations.

2. Results and discussion

2.1. PXRD analysis

Powder X-ray diffraction (PXRD) [Rigaku - SmartLab X-Ray Diffractometer, Japan- Cu$K\alpha_1$ as the X-ray source ($\lambda = 1.5407$ Å), step precision $\pm$ 0.001°] has been performed so as to undertake the spectral analysis of the TGS samples in order to understand

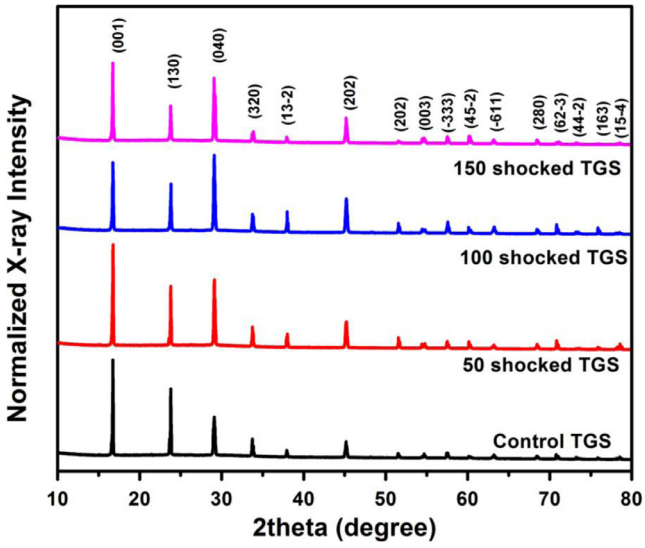

Fig. 1. Powder XRD pattern of the control and shock wave loaded TGS samples.

the effect of shock waves on their structural properties as well as structural dynamics since there could be lots of changes that would occur at shock-wave-loaded conditions. However, special attention has been given to monitor the structural properties and the obtained PXRD data of the ambient and shock-wave-loaded TGS samples are presented in Fig. 1. At the ambient condition, TGS belongs to the monoclinic crystal system with $P2_1$ space group and it is ferroelectric in nature. The observed PXRD diffraction profile of the control TGS sample is found to be consistent with the $P2_1$ crystal structure [34,35]. The XRD pattern of the control TGS sample (Fig. 1) is found to be well-matched with the earlier publications of TGS sample [34] and JCPDS card number 15–0947. The control TGS sample has sharp diffraction peaks indicating good crystallinity and the observed diffraction peaks are indexed as (001), (130), (040), (320), (13–2), (202), (003), (−333), (45–2), (−611), (280), (62–3), (44–2), (163) and (15–4). Moreover, the most predominant crystalline plane of the control sample (001) has the highest peak intensity as compared to the other crystalline peaks which may be due to the specific orientation growth enabled by the VASR technique.

Figure 1 also shows the shock-wave-loaded TGS samples' XRD patterns and from the obtained XRD patterns, it is authentic that all the original peaks of the control sample are intact after shock-wave experiments as well. Magnifying selected diffraction peaks has illustrated significant changes within the structures. In order to arrive at a clear authentication of the shock-wave impacted structural changes, the obtained XRD patterns are normalized (with 0 to 1 intensity) that are presented in Figs. 2 and 3. At first, we have to consider the most significant diffraction peak of the (001) crystal plane for the evaluation of the impact of shock waves and the corresponding diffraction patterns are presented in Fig. 2a.

As seen in Fig. 2a, the control sample has a sharp diffraction peak and nearly the same pattern is reproduced at 50 shocks with a slight peak broadening. Whereas after 100 and 150 shocks, the nature of the peak looks quite different compared to the control and 50 shocked samples. After 100 as well as 150 shocks, there is a clear formation of shoulder peaks and it illustrates that there a change in the local symmetry of TGS molecules and formation of micro-distortions in the TGS crystal system [19]. The structure of TGS crystal has three glycine molecules denoted by GI, GII and GIII, of which GI is associated with H_2SO_4. Moreover, it should be noted that among the three glycine molecules, the GI molecule has a weak hydrogen bond network while the other two molecules have strong hydrogen bonds to the skeleton molecule [36]. Under shocked conditions, there is a possibility of rotational disorder for NH_3 in the GI molecule so that it may deviate from the original angle along with the b-axis towards the quasi-planar axis. Since the GI molecule has a weak hydrogen bond network it can be easily altered with the shock-wave-impulsion. On the other hand, the GI molecule has lower activation energy (2.7 k cal/Mol) compared to the other two glycine molecules (3.9 k cal/Mol) [37]. Hence, the symmetry and ordering coefficient of the GI molecule have a greater possibility to be affected by the shock wave impacts. In the case of the (130) plane, a few shoulder peaks are eliminated whereas a few other shoulder peaks are generated due to the exposure of shock waves. This may be owing to the deformation of TGS crystalline plane by the impact of shock waves. Moreover, NH_3 is free for rotation under high-pressure conditions which has been very well reported by several researchers working on high pressure [25–28]. We attribute these new features to the abnormal rotations that might have happened in the NH_3 molecule under shocked conditions that may be the major reason for the formation of shoulder peaks. Following the (001), (130) and (040) planes also show similar results and the corresponding XRD patterns are portrayed in Fig. 2c.

Figure 3a shows the (003) and (−333) crystalline planes of the control and shock-wave- loaded TGS samples, respectively. As seen in Fig. 3a, the (003) plane of the control sample has the superposition of two moderate-intensity peaks. After shock waves are loaded (50 and 100 shocks), the (003) peak has better sharpness compared to the control sample. Surprisingly, at 150 shocks loaded conditions, the sharp peak comes back to the original shape as that of the control along with a few extra shoulder peaks and the corresponding planes are marked by red circles in Fig. 3a. (−333) plane also shows more or less similar effects as that of (003). Henceforth, it could be confirmed that the NH_3 molecule has undergone a rotational effect by the shock wave impulsion. It could be noted that the rotational angle is associated with the transient pressure and the number of applied shock pulses. Fig. 3b clearly shows that the shoulder peaks appear and disappear because of the shock-wave-impulsion in (44–2), and (15–4). But in the case of (163) plane at 50 shocks loaded conditions, the peak intensity completely disappears and appears again at 100 and 150 shocks. It could be noted that the higher-angle diffraction peaks exhibit the order- disorder - like structural changes according to the rate of exposed shock pulses and such kind of order-disorder changes are usual for sulfate materials at high-pressure conditions [25–28]. On the other hand, the polarized axis (b-axis) has hydrogen bonds that can be thermally activated above the Curie temperature and as a result, there could be the possibility of different crystallographic orientations. As per the previous assessments and observed results, the test sample exhibits a phase-transition behavior whereas our observed changes are not well-matched with the high-pressure phase [25–28] but, lots of structural disorders and deformations have materialized by the impact of shock waves. Our previous results are also well corroborated with the present observed results [30]. Among all the observed diffraction peaks, (001) is quite stable compared to other diffraction peaks due to the strong correlation with the GII and GIII functional groups (in the ac plane).

As per the analogies of the previous research publications, it is proposed that the ferroelectric nature is expected to reduce by the shock-wave impulsion because of the collapse of ferroelectric domains [25]. The values of lattice parameters have been refined by UNITCELL program and the respective values of the control and shocked samples are presented in Table 1 which exhibits that the values of the unit-cell dimensions as well as the volume are changed according to the number of exposed shock pulses that indicates the rotation of NH_3 molecule under shocked conditions. As per the values of calculated lattice parameters, the values of a,

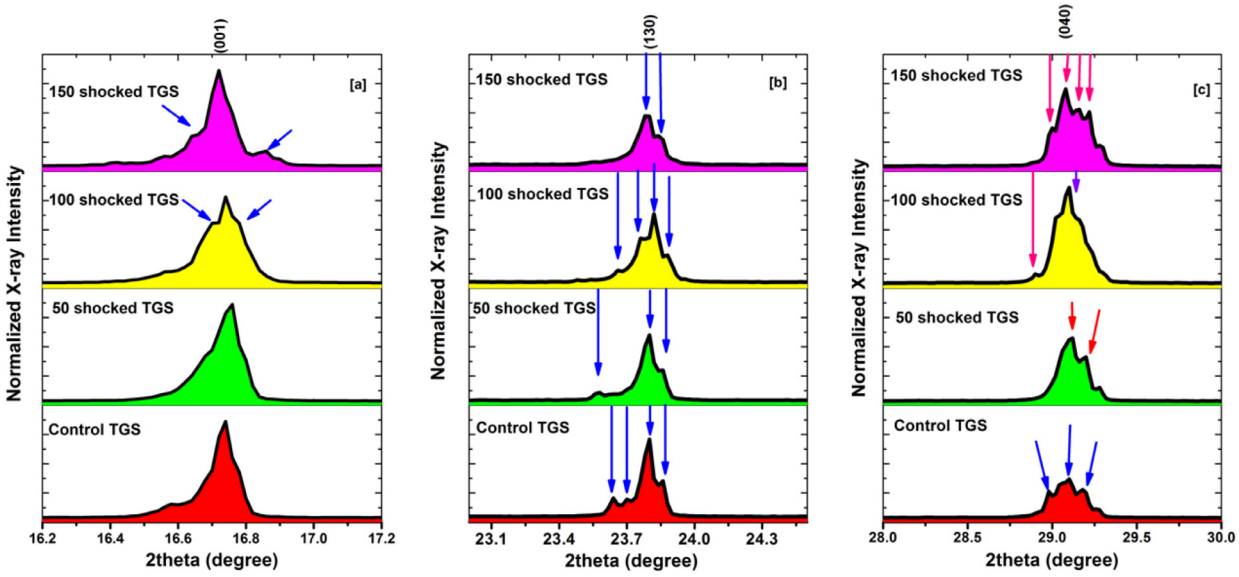

Fig. 2. Selected planes of the control and shocked TGS powder sample (a) (001) plane (b) (130) plane (c) (040) plane.

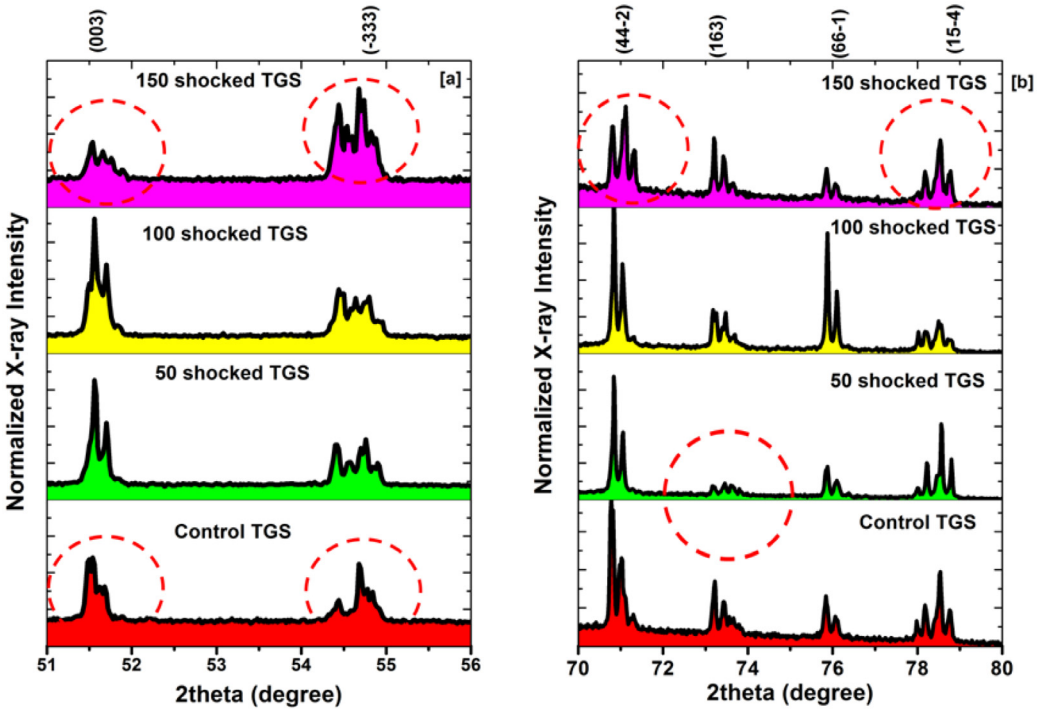

Fig. 3. XRD patterns of selected regions for the control and shocked samples (a) 51- 56° (b) 70–80°.

Table 1
The values of Lattice parameters of the control and shocked TGS samples.

Samples	Lattice parameters				
	a (Å)	b (Å)	c (Å)	V(Å)	Beta (°)
Control TGS	9.691(8)	12.573 (15)	5.754 (3)	658	115.30 (7)
50 shocked TGS	9.427 (7)	12.292 (12)	5.851(3)	674	115.41 (7)
100 shocked TGS	9.427 (7)	12.295 (14)	5.825 (3)	672	115.26 (7)
150 shocked TGS	9.417 (9)	12.132 (18)	5.463 (7)	631	112.53 (13)

b axes are reduced under shocked conditions whereas the c-axis is increased at 50 and 100 shocks but reduced at 150 shocks. Similar results have been found in previous static high-pressure experiments [25–28].

2.2. Raman analysis

On the one hand, Raman measurements are quite interesting to probe the structural phase changes and structural deformations of the test materials, especially for high-pressure experiments. On the other hand, it would be fascinating to probe the crystallographically indistinguishable ions which are spectroscopically distinct and detectable. Hence, considering the obtained results of XRD in the present experiment, Raman measurement is highly desirable to understand better the structural changes by the shock-wave impulsion. Consequently, significant effort has been expended to monitor the structural changes in TGS crystal by the shock-wave impulsion and the observed Raman spectra at room temperature for the control and shocked TGS samples are depicted in Fig. 4. The control Raman spectrum of TGS is well corroborated with the previous reports [35,38]. A Renishaw model Raman spectrometer with Laser line 532 nm and power 50 mW has been used in this study.

A majority of TGS Raman bands have been retained even after the shock- wave impulsion. So that it could be confirmed that there is no structural phase transition to occur because of the of shock-wave impact. As seen in Fig. 4, in the wavenumber region of 100-2000 cm^{-1}, we could notice changes in Raman intensity for a few of the Raman bands and also could find that a few new Raman bands have appeared owing to the impact of shock waves. At this stage, it is essential to take into account the observed changes to correlate the XRD results. Table 2 notes the presence and absence of Raman bands for the samples of pre-shocked and post-shocked.

At 50 shocks, there is a strong and intense Raman band at 1872 cm^{-1} for the control sample whereas no significant changes are observed in Raman band intensity at shocked conditions. Furthermore, at 100 shocked conditions, Raman bands of 127 and 360 cm^{-1} appear whereas all the existing Raman bands between 1000 and 1600 cm^{-1} have almost disappeared by the shock waves. Interestingly, at 150 shock-wave-loaded conditions, a

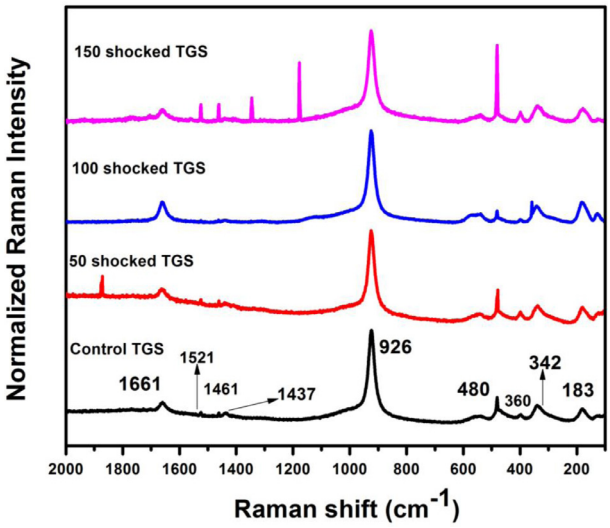

Fig. 4. Raman spectra of the control and shocked TGS samples.

few Raman bands such as 480, 1461 and 1524 cm^{-1} are dramatically enhanced in Raman intensity . On the other hand, Raman bands at 1179 and 1342 cm^{-1} which belong to NH_3 and CH_2 vibrations, respectively, have newly appeared because of the shock waves. For a better understanding of the observed results, the selected wavenumbers of Raman spectra are presented in Fig. 5 and the obtained interesting changes are marked with red circles.

Various parameters must be taken into account for a better realization of the changes observed in Raman bands such as thermally activated hopping motions of NH_3 ions, the role of hydrogen bonds in the complex crystal structure, intermolecular interaction, activation energies of three different glycine molecules etc. [37]. It is essential to understand that the Raman intensity redistribution occurs in accordance with the number of shock pulses because of the changes in the glycine molecules either in Gly-I, Gly-II or in Gly –III. But as per the literature survey, among the three glycine molecules, Gly-I has a very weak hydrogen bond network and lower activation energy (Stankowski, 1978). However, at

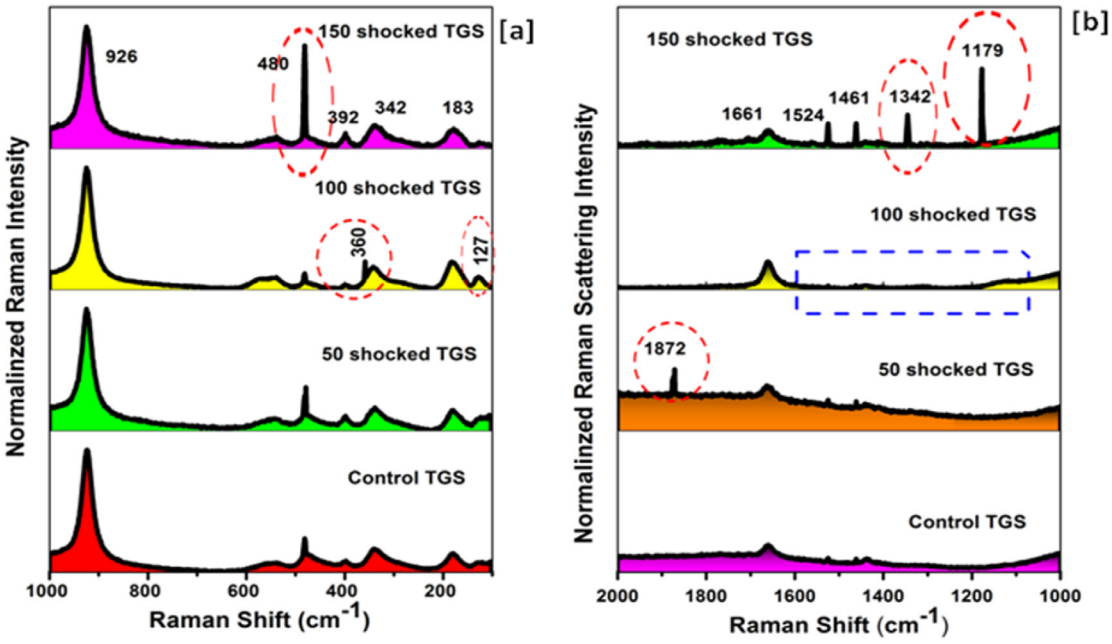

Fig. 5. Selected wavenumbers of Raman spectra of the control and shocked samples (a) 100-1000 cm^{-1} (b) 1000-2000 cm^{-1}.

Table 2
Tentative Raman band assignments of the pre-shocked and post-shocked TGS samples.

Experimental Conditions				Tentative Raman Assignments (Preeti, et al., 2018; Bajpai, & Verma, 2012)
Control TGS	50 shocks	100 shocks	150 shocks	
–	–	127	–	Lattice mode of TGS
183	183	183	183	Lattice mode of TGS
342	342	342	342	Glycine δ_{CCN}
–	–	360	–	Not assigned
392	392	392	392	CCN (Gly- III)
480	480	480	480	COO
926	926	926	926	SO_4
–	–	–	1179	NH_3 (Gly-I/Gly-III)
–	–	–	1342	CH_2
1437	1437	1437	1437	CH_2
1461	1461	1461	1461	CH_2
1524	1524	1524	1524	NH_3 (Gly-I)
1661	1661	1661	1661	C = O
–	1872	–	–	Not assigned

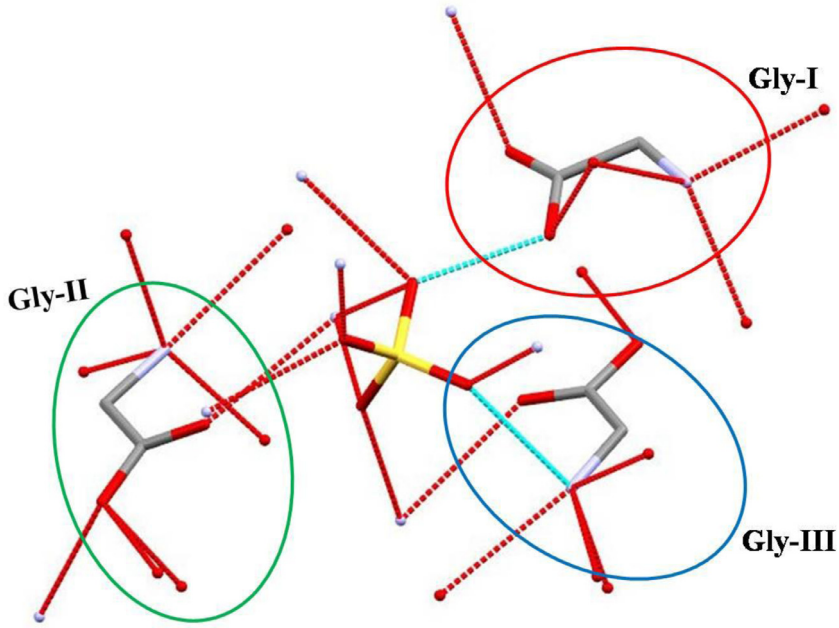

Fig. 6. Molecular structure of TGS obtained by CIF (1,270,327).

high-temperature and high-pressure conditions, there is a greater chance of re-orientation of the atomic band patterns that might induce a few changes in the actual lattice symmetry. Hence, various re-orientations could be observed with respect to temperature and pressure (Sivakumar, 2022, Frech, 1983). Such kind of re-orientations (Gly-I – NH_3_COO) may lead to the appearance and disappearance of Raman peaks by the shock-wave impulsion which is evidenced by the changes observed in the higher wavenumber of NH_3 Raman bands. On the other hand, due to the influence of shock waves, the realignment of glycine dipoles would enforce the re-orientation of glycine ions and the resultant effect would affect the intensity distribution of modes associated with it. From the Raman measurement, it is clear that there is no phase change observed by the shock waves. The XRD and Raman measurements have provided authenticated evidence for the lattice distortion of the test sample while retaining the same crystal structure under the shock-wave impacts.

3. Conclusion

Summarizing the present experimental work, the systematic analysis of shock-wave- induced structural properties of TGS sample has been carried out by employing X-ray diffraction and Raman spectroscopic methods. XRD and Raman measurements show that the test crystal has not experienced any crystallographic phase transition by the impact of shock waves. But in XRD, we have observed several shoulder peaks appearing while Raman data confirm a few new Raman bands appearing and a few existing peaks disappearing under shocked conditions. We attribute these new features to the disorder of NH_3 ions in the glycine molecule due to the weaker hydrogen-bond network. The conclusion of the present experiment is made by the observed results in such a way that the test crystal has a stable crystallographic structure quantitatively whereas it is qualitatively unstable to a small extent against the shock-wave impacts. Hence, the authors suggest performing ferroelectric studies on the test crystal against the shock waves. Since it is one of the active ferroelectric and NLO crystals, under shocked conditions significant changes in ferroelectric property are expected for TGS which will lead to a better understanding of the structure-property relationship against the shock-wave impacts. Further, shock-wave-recovery experiments along with theoretical works are highly required for NLO crystals so as to find better shock-resistant materials for the next generation of applications.

Compliance with ethical standards

None.

Declaration of competing interest

The authors declare that they have no conflict of interest.

CRediT authorship contribution statement

A. Sivakumar: Conceptualization, Investigation, Writing – original draft. **A. Saranraj:** Methodology. **S. Sahaya Jude Dhas:** Writing – review & editing. **T. Vasanthi:** Resources. **V.N. Vijayakumar:** Visualization. **P. Sivaprakash:** Resources. **V. Pushpanathan:** Formal analysis. **S. Arumugam:** Formal analysis. **Lidong Dai:** Validation. **S.A. Martin Britto Dhas:** Supervision, Writing – review & editing.

Data availability

Data will be made available on request.

Acknowledgement

The authors thank Department of Science and Technology (DST), India, for funding through DST-FIST program (SR/FST/College-2017/130 (c)). The authors thank Abraham Panampara Research Fellowship and NSF of China (42072055).

References

[1] K. Vijay Reddy, Chuang Deng, Pal Snehanshu, Dynamic characterization of shock response in crystalline-metallic glass nanolaminates, Acta Mater. 164 (2019) 347–361.
[2] Nagarajan Kirupakaran Gopinath, Gopalan Jagadeesh, Bikramjit Basu, Shock wave-material interaction in ZrB 2–SiC based ultra high temperature ceramics for hypersonic applications, J. Am. Ceram. Soc. 00 (2019) 1–14.
[3] S. Kalaiarasi, A. Sivakumar, S.A. Martin Britto Dhas, M. Jose, Shock wave induced anatase to rutile TiO_2 phase transition using pressure driven shock tube, Mater. Lett. 219 (2018) 72–75.
[4] A. Sivakumar, S. Suresh, S. Balachandar, J. Thirupathy, J. Kalyana Sundar, S.A. Martin Britto Dhas, Effect of shock waves on thermophysical properties of ADP and KDP crystals, Opt. Laser. Tech. 111 (2019) 284–289.
[5] Yuying Yu, Ye Tan, Chengda Dai, Xuemei Li, Yinghua Li, Qiang Wu, Hua Tan, Phase transition and strength of vanadium under shock compression up to 88GPa, Appl. Phys. Lett. 105 (2014) 201910.
[6] N. Koteeswara Reddy, V. Jayaram, E. Arunan, Y.B. Kwon, W.J. Moon, K.P.J. Reddy, Investigations on high enthalpy shock wave exposed graphitic carbon Nanoparticles, Diam. Relat. Mater 35 (2013) 53–57.
[7] A. Sivakumar, C. Victor, M. Muralidhr Nayak, S.A. Martin Britto Dhas, Structural, optical, and morphological stability of ZnO nano rods under shock wave loading conditions, Mater. Res. Express 6 (2019) 045031.
[8] V. Jayaram, K.P.J. Reddy, Experimental study of the effect of strong shock heated test gases with cubic zirconia, Adv. Mater. Lett. 7 (2016) 100–150.
[9] A. Sivakumar, A. Saranraj, S. Sahaya Jude Dhas, S.A. Martin Britto Dhas, Shock wave induced enhancement of optical properties of Benzil crystal, Mater. Res. Express 6 (2019) 046205.
[10] A. Sivakumar, S.A. Martin Britto Dhas, Shock-wave-induced nucleation leading to crystallization in water, J. Appl. Cryst. 52 (2019) 1016–1021.
[11] Satish C. Gupta, S.K. Sikk, Some investigations on shock wave induced phase transitions, Shock Waves 6 (1996) 345–359.
[12] Shockinduced phase transformation in lithium niobate; Tsueneaki Goto and Yasuhiko Syono, J. Appl. Phys. 58 (1985) 2548.
[13] M. Devika, N.Koteeswara Reddy, V. Jayaram, K.P.J. Reddy, Sustainability of aligned ZnO nanorods under dynamic shock-waves, Adv. Mater. Lett. 8 (2017) 398–403.
[14] D. Choudhuri, Y.M. Gupta, Shock compression of aluminum single crystals to 70GPa: role of crystalline anisotropy, J. Appl. Phys. 114 (2013) 153504.
[15] A. Sivakumar, S. Balachandar, S.A. Martin Britto Dhas, Measurement of "Shock Wave Parameters" in a novel table-top shock tube using microphones, Hum. Fact. Mech. Engg. Defense. Saf. 4 (2020) 3.
[16] Jiyang Wang, Haohai Yu, Yicheng Wu, Robert Boughton; Recent developments in functional crystals in china, Engineering 1 (2015) 192–210.
[17] A. Sivakumar, et al., X-ray and Raman scattering measurements of ammonium dihydreogen phophaste crystal at shocked conditions, Z. Crystl. Mater (2020).
[18] A. Sivakumar, S. Sahaya Jude Dhas, S. Balachandar, S.A. Martin Britto Dhas, Impact of shock waves on molecular and structural response of potassium dihydrogen phosphate crystal 48 (2019) 7868–7873.
[19] A.N. Zhukova, N.S. Sidorovb, A.V. Palnichenkob, V.V. Avdonina, D.V. Shakhrai, Influence of shock-wave pressure up to 65GPa on the crystal structure and superconducting properties of MgB_2, High Press. Res. 29 (2009) 414–421.
[20] Jiann-Min Chang, Ashok K. Batra, Ravindra B. La, Growth and characterization of doped TGS crystals for infrared devices, Crystal. Growth . Design 2 (2002) 431–435.
[21] H.V. Alexandru, Pure and doped triglycine sulfate crystals growth and characterization, Interdiscip. Transp. Phenomena: Ann. N.Y. Acad. Sci. 1161 (2009) 387–396.
[22] C. Berbecarua, H.V. Alexandrua, L. Pintilieb, A. Dutua, B. Logofatua, R.C. Radulescu, Doped versus pure TGS crystals, Mater. Sci. Eng. B 118 (2005) 141–146.
[23] P.R. Deepthia, J. Shanthi, Optical, dielectric & ferroelectric studies on amino acids doped TGS single crystals, RSC Adv. 6 (2016) 33686–33694.
[24] R.B. Lal, A.K. Batra, Growth and poperties of Triglycine Sulfate (TGS) crystals: review, Ferroelectrics 142 (1993) 51–82.
[25] B. Andriyevsky, W. Ciepluch-Trojanek, A. Patryn, Effect of hydrostatic pressure on structural and electronic properties of TGS crystals (first-principle calculations), Cond. Matt. Phys 10 (2007) 33–38.
[26] J. Stankowski, S. Waplak, Damage to TGS crystals caused by hydrostatic pressure, Mater. Sci.-Poland 27 (2009) 249–253.
[27] Y. Kobayashi, S. Sawada, H. Furuta, S. Endo, K. Deguchi, Ferroelectric TGS ($(NH_2CH_2COOH)_3 \cdot H_2SO_4$) under high pressure, J. Phys. Cond. Matt 14 (2002) 11139–11142.
[28] Eisuke Suzuki, Yuki Kobayashi, Shoichi Endo, Kiyoshi Deguchi, Takumi Kikegawa, Pressure-induced structural transition in TGS, Ferroelectrics 285 (2003) 167–172.
[29] J. Stankowski, A. Gaxqzewski, S. Waplak, U. Cruszczfiska, H. Gierszal, dielectric properties of TGS and TGFB Monocrystals under high pressure, Ferroelectrics 6 (1974) 209–214.
[30] A. Sivakumar, A. Saranraj, S. Sahaya Jude Dhas, M. Jose, S.A. Martin Britto Dhas, Shock wave-induced defect engineering for investigation on optical properties of triglycine sulfate crystal, Opt. Eng. 58 (2019) 077104.
[31] A. Saranraj, A. Jenipriya, S. Sahaya Jude Dhas, M. Jose, S.A. Martin Britto Dhas, Vacuum-assisted technique to modify the sr method for unidirectional crystal growth, Cryst. Res. Technol. 53 (2018) 1700255.
[32] A. Sivakumar, S. Balachandar, S.A. Martin Britto Dhas, Measurement of "shock wave parameters" in a novel table-top shock tube using microphones, Hum. Fact. Mech.Engg. Defense. Saf. 4 (2020) 3.
[33] A. Sivakumar, S. Sahaya Jude Dhas, S. Balachandar, S.A. Martin Britto Dhas, Effect of shock waves on structural and dielectric properties of ammonium dihydrogen phosphate crystal, Z. Kristallogr. 234 (2019) 557–567.
[34] Abid Hussain, Nidhi Sinha, Abhilash J. Joseph, Sahil Goel, Budhendra Singh, Igor Bdikin, Binay Kumar, Mechanical investigations on piezo-/ferroelectric maleic acid-doped triglycine sulphate single crystal using nanoindentation technique, Arabian J. Chem. 13 (2020) 1874–1889.
[35] Preeti Singh, M.M. Abdullah, Suresh Sagadevan, Saiqa Ikram, Enhancement of electro-optic and structural properties of TGS single crystals on doping with L-glutamic acid, J. Mater. Sci.: Mater. Electron. 29 (2018) 7904–7916.
[36] R.R. Choudhury, R. Chitra, P.U. Sastry, Amit Das, M. Ramanadham, Phase transition in triglycine family of hydrogen bonded ferroelectrics: an interpretation based on structural studies, Pramana. J. Phys- 63 (2004) 107–115.
[37] J. Stankowski;, Radiospectroscopic studies of ferroelectric triglycine sulphate–like crystals. Radiospectroscopic studies of ferroelectric Triglycine sulphate-like crystals, Ferroelectrics 20 (1978) 109–120.
[38] P.K. Bajpai, A.L. Verma, Molecular dynamics of glycine ions in alanine doped TGS single crystal as probed by polarized laser raman spectroscopy, Spectrochim Acta A 96 (2012) 906–915.